



## LJMU Research Online

**Buffey, AJ, Onambélé-Pearson, GL, Erskine, RM and Tomlinson, DJ**

**The validity and reliability of the Achilles tendon moment arm assessed with dual-energy X-ray absorptiometry, relative to MRI and ultrasound assessments.**

<http://researchonline.ljmu.ac.uk/id/eprint/14289/>

### Article

**Citation** (please note it is advisable to refer to the publisher's version if you intend to cite from this work)

**Buffey, AJ, Onambélé-Pearson, GL, Erskine, RM and Tomlinson, DJ (2020) The validity and reliability of the Achilles tendon moment arm assessed with dual-energy X-ray absorptiometry, relative to MRI and ultrasound assessments. Journal of Biomechanics. 116. ISSN 1873-2380**

LJMU has developed [LJMU Research Online](#) for users to access the research output of the University more effectively. Copyright © and Moral Rights for the papers on this site are retained by the individual authors and/or other copyright owners. Users may download and/or print one copy of any article(s) in LJMU Research Online to facilitate their private study or for non-commercial research. You may not engage in further distribution of the material or use it for any profit-making activities or any commercial gain.

The version presented here may differ from the published version or from the version of the record. Please see the repository URL above for details on accessing the published version and note that access may require a subscription.

For more information please contact [researchonline@ljmu.ac.uk](mailto:researchonline@ljmu.ac.uk)

<http://researchonline.ljmu.ac.uk/>

1 **The validity and reliability of the Achilles tendon moment arm assessed with Dual-energy**  
2 **X-ray absorptiometry, relative to MRI and ultrasound assessments**

3 Aidan J. Buffey<sup>1, 2, 3</sup>, Gladys L. Onambélé-Pearson<sup>1</sup>, Robert M. Erskine<sup>4, 5</sup> and David J.  
4 Tomlinson<sup>1</sup>

5  
6 <sup>1</sup>*Musculoskeletal Science and Sports Medicine Research Centre, Manchester Metropolitan*  
7 *University, Manchester, UK ;* <sup>2</sup>*Department of Physical Education and Sport Sciences;*  
8 *University of Limerick, Limerick, Ireland;* <sup>3</sup>*Health Research Institute, University of Limerick,*  
9 *Limerick, Ireland;* <sup>4</sup>*Research Institute for Sport & Exercise Sciences, Liverpool John Moores*  
10 *University, Liverpool, UK;* <sup>5</sup>*Institute of Sport, Exercise & Health, University College London,*  
11 *London, UK.*

12  
13 **Address for reprint requests and all other correspondence:**

14 \*Dr David J. Tomlinson, Department of Sport and Exercise Sciences, Musculoskeletal Science  
15 and Sports Medicine Research Centre, Manchester Metropolitan University, Manchester, M1  
16 5GD, United Kingdom; Telephone: +44 (0)161 247 5594; Email:  
17 david.tomlinson@mmu.ac.uk

18  
19  
20  
21 **This is an original article**

22  
23 Word Count: 3758

24 Keywords: Achilles tendon; Moment arm; Dual-energy X-ray absorptiometry; Magnetic  
25 resonance imaging; Tendon excursion

26 **Abstract**

27 Dual-energy X-ray absorptiometry (DXA) in single energy mode has been shown to permit the  
28 visualisation of bone and soft tissue, such as the patellar tendon through two-dimensional  
29 sagittal imaging. However, there is no validated DXA-based measurement of the Achilles  
30 tendon moment arm ( $d_{AT}$ ). The aims of this study were: 1) to compare *in vivo* DXA derived  
31 measurements of the  $d_{AT}$  at rest against two previously validated methods: tendon excursion  
32 (TE) and magnetic resonance imaging (MRI) at three ankle angles ( $-5^\circ$ ,  $0^\circ$  and  $+10^\circ$ ). 2)  
33 analyse the intra-day reliability of the DXA method at all ankle angles and compare between  
34 methods. Twelve healthy adults (mean $\pm$ SD: 31.4 $\pm$ 9.5 years; 174.0 $\pm$ 9.5 cm; 76.2 $\pm$ 16.6 kg)  
35 participated in this study, involving test-retest DXA scans, ultrasound scans and one MRI scan.  
36 The  $d_{AT}$  was defined as the distance from the centre of the calcaneal-tibial joint axis to the  
37 Achilles tendon (AT) muscle-tendon line of action. DXA derived  $d_{AT}$  measures were  
38 significantly greater than MRI measurements (19.7-24.9%) and were 45.2% significantly  
39 larger than the TE method. The test-retest reliability of the DXA technique at  $0^\circ$  was high  
40 [CV=1.38%; ICC=0.96] and despite the consistently larger  $d_{AT}$  lengths obtained using DXA,  
41 MRI and DEXA data were strongly correlated ( $r=0.878$ ,  $p<0.001$ ). In conclusion, the DXA  
42 technique allowed for highly reproducible *in vivo*  $d_{AT}$  measurement at rest, which has  
43 implications for the calculation of AT forces *in vivo* and the ability to predict the measurement  
44 from one tool to the other, thereby providing a novel basis to contrast existing and future studies.

45

46

47

48

49

50

## 51 **Introduction**

52

53 The Achilles tendon moment arm ( $d_{AT}$ ) is a measure widely used within biomechanics and  
54 important when converting individual muscle forces from the *gastrocnemius* (GM) and *soleus*  
55 into a moment about the ankle or vice versa (Clarke et al., 2015; Maganaris et al., 1998; Rasske  
56 et al., 2017).  $d_{AT}$  length is defined as a perpendicular distance from the ankle joints axis of  
57 rotation to the Achilles tendon (AT) muscle-tendon line of action (Fletcher and MacIntosh,  
58 2018; Maganaris, 2003; Sheehan, 2012). Its length has implications both clinically and  
59 experimentally as it can relate joint torques and muscle forces, with the  $d_{AT}$  vital in  
60 musculoskeletal modelling (Clarke et al., 2015; Maganaris, 2004; Maganaris et al., 1998;  
61 Sheehan, 2012). Accurate measurement of the  $d_{AT}$  length is important when discussing the  
62 muscle-tendon at the ankle joint as larger  $d_{AT}$  lengths allow for greater muscle-tendon  
63 displacement, velocities and larger joint moments (Maganaris, 2004).

64 Reliable and valid methods are required when obtaining parameters such as  $d_{AT}$  which proves  
65 difficult due to the complex nature of defining the axis of rotation (Alexander et al., 2017) and  
66 determining the line of action. Numerous techniques have been implemented in the  
67 measurement of  $d_{AT}$  *in vivo* such as magnetic resonance imaging (MRI) and ultrasound imaging  
68 as the accuracy and repeatability associated with medical imaging techniques surpass the  
69 simplicity of surface measurements and cadaver tissue (Alexander et al., 2017; Wilson et al.,  
70 1999). The ultrasound and MRI techniques have become common practice in the measurement  
71 of the  $d_{AT}$  (Fath et al., 2010). Whereas, to our knowledge, dual-energy X-ray absorptiometry  
72 (DXA), has yet to be routinely utilised in the measurement of  $d_{AT}$ . However, DXA under single  
73 energy mode has been shown to produce two-dimensional (2D) sagittal images that permit the  
74 visualisation of bone and soft tissue with high water content, formerly validated against MRI  
75 in the patellar tendon moment arm ( $d_{PT}$ ) (Erskine et al., 2014). With a ‘high definition instant

76 vertebral assessment' (IVA-HD) DXA protocol, high-quality sagittal images of the knee joint  
77 allowed the  $d_{PT}$  to be measured when rested at full extension (Erskine et al., 2014).

78 MRI provides high visibility of the anatomical structure capturing bony configurations of the  
79 calcaneal-tibial joint, depicting soft tissue and allowing the line of action to be easily identified  
80 (Fath et al., 2010; Fletcher and MacIntosh, 2018; Hashizume et al., 2012; Rugg et al., 1990).

81 This permits  $d_{AT}$  to be measured directly without erroneous assumptions regarding the actual  
82 path of the tendon (Rugg et al., 1990). With MRI,  $d_{AT}$  is estimated as a distance using the  
83 centre of rotation (COR) technique where the distance from the joint axis to the muscle-tendon  
84 line of action is measured (Rugg et al., 1990). The ultrasound technique termed tendon  
85 excursion (TE) operates without clear identification of the joint COR or muscle-tendon action  
86 line, providing an estimation of  $d_{AT}$  length (Fath et al., 2010). TE calculates  $d_{AT}$  during passive  
87 rotation of the ankle as the ratio of tendon displacement at the musculotendinous junction (MTJ)  
88 to joint rotation (Fletcher and MacIntosh, 2018).

89 Since no previous study has measured  $d_{AT}$  utilising DXA, the opportunity to directly compare  
90 the three techniques discussed above *in vivo* has not been available. The ability to utilise DXA  
91 in the measurement of  $d_{AT}$  is advantageous, as the novel method proposed, would be quicker,  
92 cheaper and more accessible compared to an MRI and allows the calculation of  $d_{AT}$  length  
93 whereas TE provides an estimation of  $d_{AT}$  length. Therefore, by directly comparing DXA, MRI  
94 and ultrasound a comparison can be provided for any measurement differences, which is  
95 essential when looking to reliably compare results between studies (Erskine et al., 2014).

96 Furthermore, a relatively novel application of DXA  $d_{AT}$  requires validation, preferably against  
97 a recognised or the current gold standard technique such as MRI (Erskine et al., 2010;  
98 Onambele-Pearson and Pearson, 2012). The aims of the current study were twofold: 1) to  
99 investigate the *in vivo* assessment of  $d_{AT}$  at rest using: DXA, MRI and ultrasound to observe  
100 whether differences exist between the imaging protocols. 2) to determine the reliability of  $d_{AT}$

101 measurements using DXA. It was hypothesised that: 1) the intraday reliability of the DXA  
102 protocol would be high, and 2) ultrasonography would underestimate measurements made  
103 using the MRI technique and that DXA measurements would overestimate those of the MRI  
104 and ultrasound at all ankle joint angles. We hypothesised that DXA would overestimate MRI  
105 measurements of  $d_{AT}$  length as a previous study which investigated this novel DXA method  
106 found DXA to overestimate MRI when comparing measurements of the  $d_{PT}$  (Erskine et al.,  
107 2014). Similarly, we hypothesised ultrasonography or the TE method to underestimate MRI  
108  $d_{AT}$  measurements due to previous research highlighting this (Hashizume et al., 2016).

109

## 110 **Methods**

111

### 112 **Participants**

113 Twelve healthy adults (eight men and four women) were recruited to participate in this study  
114 in line with previous moment arm validation studies (Erskine et al., 2014; Hashizume et al.,  
115 2016). Age, stature and body mass (mean $\pm$ SD) were as follows: 31.4 $\pm$ 9.5 years, 174.0 $\pm$ 9.5 cm,  
116 and 76.2 $\pm$ 16.6 kg, respectively. Participants self-reported as physically active and free of lower  
117 limb musculoskeletal injuries, ankle joint/AT disorders with no history of ankle surgery and  
118 not pregnant (relating to the radiation exposure during the DXA scan). Participants provided  
119 written informed consent before participating in this study, which conformed with the  
120 Declaration of Helsinki (World Medical, 2013). This study was approved by the local ethics  
121 committee of Manchester Metropolitan University.

122

### 123 **Experimental Protocol**

124 Over two laboratory visits the participants  $d_{AT}$  of their right ankle was quantified using three  
125 techniques. On the first laboratory visit, the participants  $d_{AT}$  was assessed twice using a

126 Discovery W DXA scanner [Hologic Inc., Bedford, USA] to allow the reliability of the DXA  
127 protocol to be investigated, and assessed once using ultrasonography [Esaote Biomedica,  
128 Genoa, Italy]. On the second laboratory visit, 24 hours later, the participants  $d_{AT}$  was measured  
129 once using a 0.25-T G-Scan MRI scanner [Esaote Biomedica, Genoa, Italy].

130

### 131 **Scanning Protocols**

132 For the MRI protocol, participants laid on their left side and were instructed to remain still and  
133 relaxed inside a 0.25-T G-Scan MRI scanner [Esaote Biomedica, Genoa, Italy] with their right  
134 knee extended (Figure 1a). The sole of the right foot was positioned against a custom-made  
135 wooden device, with the ankle secured to the device using two non-elastic Velcro straps. The  
136 custom-made device allowed manipulation of the ankle and fixed the angle of the ankle joint  
137 for the subsequent scans ( $-5^\circ$ ,  $0^\circ$  and  $+10^\circ$ ). Sagittal ankle scans were acquired using a Turbo  
138 3D T1-weighted sequence with the following scanning parameters: time of repetition=40 ms;  
139 time to echo=16 ms; matrix=256 x 256; field of view=180 mm x 180 mm; slice thickness=3.4  
140 mm; interslice gap=0 mm.

141

142 [Insert Figure 1]

143

144 For the DXA session, six single energy IVA-HD scans [Hologic Inc., Bedford, USA] with the  
145 participant lying on their right side (Figure 1b) were taken at the three pre-determined ankle  
146 joint angles, with two scans taken per joint angle ( $-5^\circ$ ,  $0^\circ$  and  $+10^\circ$ ). The right ankle was  
147 manipulated and fixed at these angles using the same custom-made wooden device utilised in  
148 the MRI protocol (Figure 1b). The IVA-HD parameters were as follows: scan length=20.3 cm;  
149 scan width=13.7 cm; line spacing=0.0241 cm; point resolution=0.1086 cm; scanning time=11 s.  
150 The acquired sagittal images of the participant's right ankle were attained by placing the ankle

151 joint with the lateral aspect of the limb within the imaging zone. To enable the reliability of  
152 IVA-HD DXA scans to be analysed, the procedure was repeated, which required participants  
153 to be removed and then repositioned back on the scanner in between DXA scans.

154 For the TE protocol, participants were seated on an isokinetic dynamometer [Cybex Norm,  
155 Cybex International, New York, USA] with their right ankle securely fixed with inextensible  
156 straps. The right knee was fully extended with the right thigh strapped to the dynamometer  
157 chair (Figure 1c). The participants hip angle was set to  $85^\circ$  and the participants were secured  
158 to the dynamometer at the shoulders and hip with inextensible straps. The centre of the lateral  
159 malleolus was aligned visually to the axis of rotation of the dynamometer. Participants  
160 preconditioned the muscle-tendon complex using five ramped isometric plantarflexions at 50%  
161 of self-perceived maximum (Maganaris and Paul, 1999), and then performed three maximum  
162 voluntary plantar-flexion contractions. Thereafter, the maximum range of motion (ROM) of  
163 the dynamometer was set to the participant's voluntary maximum plantarflexion and maximum  
164 dorsiflexion. To familiarise the participants, the ankle was passively rotated through the ROM  
165 limit at a constant velocity of  $1^\circ \cdot s^{-1}$  prior to assessing  $d_{AT}$ . To measure  $d_{AT}$  the ankle was  
166 passively rotated through the ROM, during which the displacement of the GM MTJ was  
167 recorded using B-mode ultrasound with a 7.5 MHz, 50 mm linear probe [Esaote AU5,  
168 Biomedica, Genoa, Italy]. The probe was fixed in position using a custom-built foam cast. To  
169 ensure accurate measurements of displacement, a 2 mm echo-absorptive tape was placed over  
170 the MTJ at  $0^\circ$  ankle position to check for movement of the probe. If any movement was detected  
171 the test was repeated. This procedure was repeated to measure the reliability of the TE protocol,  
172 the participant was removed from the dynamometer between assessments, with all pen  
173 markings and tape removed before the measurement process was repeated.

174

## 175 **Image Analysis**



176 All DICOM images from the MRI and DXA scans were imported to a DICOM viewer [Osirix  
177 2.7.5, Osirix Foundation, Geneva, Switzerland]. For MRI scans, the midsagittal slice was  
178 identified (typically between slice 12-15) and  $d_{AT}$  was then calculated from the joint COR  
179 identified using the Reuleaux' method (see Figure 2a). The  $d_{AT}$  for the single 2D DXA DICOM  
180 image was measured as reported for the MRI analysis (see Figure 2b).

181 When analysing  $d_{AT}$  with the TE method at 0° ankle angle, the maximal plantarflexion and  
182 dorsiflexion of one ROM test was screen grabbed and analysed using ImageJ [ImageJ 1.45s;  
183 National Institutes of Health] software. The displacement of the MTJ away from the echo  
184 absorptive marker was measured at maximal plantarflexion (See Figure 2c). The total  
185 displacement was then divided by the change in the ankle angle through a full ROM  
186 (Tomlinson et al., 2014).

187

[Insert Figures 2]

189

## 190 **Statistical Analyses**

191 Statistical analysis was performed using SPSS (Version 25, SPSS Inc., Chicago, IL, USA).  
192 Data reduction reliability was confirmed using two datasets for the TE, DXA and MRI.  
193 Coefficients of variance (CVs) for the novel DXA technique were calculated between datasets.  
194 The intra class correlation coefficients (ICC, model: 2-way mixed; types: absolute agreement  
195 and consistency) were calculated for the DXA method to determine the test-retest reliability of  
196 the novel DXA method (See Table 2). The mean value of the first dataset measurements for  
197 TE, DEXA and MRI was used in the statistical analysis. Parametricity of the  $d_{AT}$  data utilised  
198 the Shapiro-Wilk test (sample normally distribution) and the Levene's test (homogeneity of  
199 variance). Thus, a repeated-measures ANOVA (rANOVA) was used to examine between-  
200 methods differences of DXA, MRI and TE with a Bonferroni correction for post hoc pairwise

201 comparisons at 0° ankle angle. An rANOVA was used to examine between-methods  
202 differences of DXA and MRI with a Bonferroni correction for post hoc pairwise comparison  
203 at -5° and 10° ankle angle. A Pearson's product-moment correlation was used to examine the  
204 associations between the DXA and MRI  $d_{AT}$  data at -5°, 0° and 10° and between TE and DXA  
205 and TE and MRI at 0°. Bland-Altman plots were developed using SPSS to illustrate the mean  
206 difference between DXA and MRI derived  $d_{AT}$  measurements; the limits of agreement were set  
207 at  $1.96 \times SD$  of the method difference. Statistical significance was accepted with  $p < 0.05$  and all  
208 data are presented as means  $\pm$  SD unless otherwise stated.

209

## 210 **Results**

211 DXA-originated  $d_{AT}$  values were consistently higher at all ankle angles measured (Table 1)  
212 than those determined from the MRI and TE techniques, especially at 0° ankle angle (Figure  
213 3). Thus at 0° ankle angle, there was a main effect of measurement method on attained  $d_{AT}$   
214 value ( $F(1,144, 12.588) = 133.571, p < 0.001$ ). Post hoc tests revealed that DXA  $d_{AT}$   
215 measurement resulted in a 19.7% greater  $d_{AT}$  measurement compared to MRI ( $p < 0.001$ ). MRI  
216  $d_{AT}$  measurement resulted in a 40.8% greater  $d_{AT}$  measurement compared to TE ( $p < 0.001$ ) and  
217 when comparing TE and DXA, DXA  $d_{AT}$  measurements were 45.2% greater than TE  $d_{AT}$   
218 measurements ( $p < 0.001$ ).

219

220 [Insert Figure 3]

221

222 There was an interaction between the DXA and MRI techniques and ankle angles  
223 ( $F(1,11) = 10.808, p = 0.007$ ). Post hoc pairwise comparison revealed that at -5° ankle angle DXA  
224  $d_{AT}$  measurements were greater (22.6%) than those derived from MRI technique ( $p < 0.001$ ) and  
225 at 10° ankle angle DXA  $d_{AT}$  measurements were larger (24.9%) than MRI ( $p < 0.001$ ).

226

227 There was a strong positive correlation between DXA and MRI ( $r=0.878, n=12, p<0.001$ ) (See  
228 Figure 4).

229

230 [Insert Figure 4]

231

232 No relationship was observed between TE and DXA ( $r=0.383, n=11, p=0.219$ ) or TE and MRI  
233 ( $r=0.293, n=11, p=0.356$ ).

234

235 The test-retest reliability of the DXA method was excellent, demonstrated by low CVs and ICC  
236 values  $>0.75$  at all ankle angles measured (See Table 2).

237 Heteroscedasticity was observed in the residuals (i.e.  $[DXA-MRI]^2$ ) between DXA and MRI  
238  $d_{AT}$  measurements) at  $-5^\circ$  ( $p=0.010$ ) and  $10^\circ$  ( $p=0.046$ ) ankle angle. At  $0^\circ$  ankle angle, the  
239 distribution of the residuals was homoscedastic, suggesting that the between method difference  
240 was not dependent on  $d_{AT}$  when measured at this ankle angle.

241 This study observed a systematic over-approximation of  $d_{AT}$  length when measured using the  
242 DXA technique compared to the MRI technique. If DXA was utilised in place of MRI, DXA  
243 would overestimate MRI  $d_{AT}$  length by 9 to 11 mm (See Figure 5a, 5b and 5c).

244

245 [Insert Figure 5]

246

## 247 **Discussion**

248 In this study, the reliability of a novel DXA technique, for the measurement of individuals  $d_{AT}$   
249 length *in vivo*, was assessed in a healthy young adult population. The main findings from this  
250 study have shown that the novel 2D DXA method produced highly reproducible  $d_{AT}$

251 measurements given its low CVs and high ICCs. Thus, to our knowledge, this shows for the  
252 first time that the DXA imaging technique enables a reliable measure of  $d_{AT}$  length. The  
253 hypothesis was accepted as the novel DXA technique gave significantly larger  $d_{AT}$   
254 measurements at all ankle angles measured when compared to the established 2D MRI method  
255 and the TE technique. Despite the consistently larger DXA  $d_{AT}$  measurements, the DXA and  
256 MRI techniques were in strong agreement irrespective of inter-individual differences in ankle  
257 joint dimensions. The agreement was shown through Bland-Altman plots and the significant  
258 positive correlation between the DXA and MRI techniques when assessing  $d_{AT}$  length, *in vivo*.  
259 A lack of association between TE vs. MRI and DXA was observed, suggesting its suitability  
260 in measuring the  $d_{AT}$  needs further analysis.

261 The novel DXA technique permitted the visualisation of the AT, allowing the measurement of  
262 individuals  $d_{AT}$ , through a single high-quality 2D sagittal image. The single energy IVA-HD  
263 scan protocol discerns soft tissue with high water content such as the AT and enables the resting  
264 ankle joint and more specifically the AT to be visualised at the investigated  $-5^\circ$ ,  $0^\circ$  and  $10^\circ$   
265 ankle angles. The sagittal images attained could depict the tibia, fibula, medial malleolus,  
266 calcaneus, talus and navicular bone clearly (Figure 2b). Hence it was possible to measure the  
267  $d_{AT}$ , i.e. the perpendicular distance from the estimated ankle joints axis of rotation to the AT  
268 muscle-tendon line of action (Maganaris et al., 2000). The visualisation of the AT through the  
269 DXA derived image compared to the MRI derived image is less clear and appears as a shadow  
270 (though distinct) image compared to the clear anatomical image provided by the MRI technique  
271 (See Figure 3a and 3b). While this may cause a small potential error in discerning the AT from  
272 the DXA sagittal images compared to MRI, we propose that a suitably trained researcher with  
273 knowledge of the AT and the anatomical image of the ankle joint will be able to discern the  
274 AT from the DXA derived sagittal image.

275 The  $29.5\pm 6.2$  mm (TE) *in vivo*,  $d_{AT}$  values reported within this study were comparable to  
276 previous findings using TE. These previous studies have reported similar  $d_{AT}$  lengths compared  
277 with our data at 32 mm (29 to 36 mm 95% confidence intervals (CI)) (Baxter and Piazza, 2018)  
278 and  $31\pm 3.7$  mm in sprinters when measuring  $d_{AT}$  with the TE technique (Lee and Piazza, 2009).  
279 However, even larger  $d_{AT}$  measurements have been reported when using the TE technique at  
280 38 mm (35 to 42 mm 95% CI) (Fath et al., 2010) and  $41.6\pm 5.5$  mm (Lee and Piazza, 2009) that  
281 would be comparable to our MRI derived  $d_{AT}$  values ( $43.3\pm 3.7$  mm (MRI)). The measurements  
282 reported using the novel 2D DXA technique,  $53.9\pm 5.2$  mm, are closely comparable to previous  
283  $d_{AT}$  values where researchers measured  $d_{AT}$  with the MRI method. Previously,  $d_{AT}$  values of 53  
284 mm (51 to 56 mm 95% CI) (Baxter and Piazza, 2018) and 54 mm (51 to 57 mm 95% (CI) (Fath  
285 et al., 2010) have been reported when measured using the MRI technique. When rationalising  
286 the larger estimations of  $d_{AT}$  length through the DXA technique, it was previously addressed  
287 that the DXA method produces a single sagittal image which represents an ‘average’ view of  
288 the calcaneal-tibial joint (Erskine et al., 2014). Whereas the MRI technique allows for analysis  
289 at a multitude of ‘slices’ in the sagittal plane, possibly accounting for some of the 19.7-24.9%  
290 difference in  $d_{AT}$  lengths between DXA and MRI at the different ankle angles as the COR point  
291 will not be identical.

292 Previous research has demonstrated that the use of dissimilar techniques such as TE and MRI  
293 as well as dissimilar methodologies when using the same technique in measuring  $d_{AT}$  has led  
294 to variances in  $d_{AT}$  estimations (Sheehan, 2012). A weak relationship was reported, in our  
295 results, when comparing the TE method to the 3D MRI protocol. Previous literature has  
296 suggested that individuals have varying AT stiffness and slack length which makes evaluating  
297 individuals  $d_{AT}$  difficult when utilising the TE technique (Baxter and Piazza, 2018; Hashizume  
298 et al., 2016). Variances in AT stiffness and slack length dictate the potential tendon elongation

299 during passive ankle movements (TE) and illustrates variability within the healthy adult cohort  
300 (Fletcher and MacIntosh, 2018; Muraoka et al., 2002).

301 Hashizume et al. (2016) reported a significant correlation between TE and 3D MRI, however  
302 reporting a correlation value of ( $p=0.05$ ,  $r^2=0.352$ ) which constitutes a ‘weak’ relationship.  
303 This finding was similarly reported by Baxter and Piazza (2018) who revealed only a positive  
304 trend ( $p=0.052$ ,  $r^2=0.21$ ) but not either a significant or a ‘strong’ relationship. This led those  
305 researchers to suggest that the TE method may not be suitable to evaluate the singular  
306 variability of individuals  $d_{AT}$  (Hashizume et al., 2016). The lack of correlation observed within  
307 our results between TE and MRI ( $p=0.356$ ,  $r^2=0.085$ ) is thus comparable to previous research  
308 (Baxter and Piazza, 2018).

309 Our results observed larger  $d_{AT}$  lengths at greater plantarflexion ankle angles, with  $-5^\circ$  ankle  
310 angle exhibiting the shortest  $d_{AT}$  length (Table 1). The novel DXA technique was shown to be  
311 highly reliable at  $0^\circ$  ankle angle, with low CV’s and high ICC’s. Both  $-5^\circ$  and  $+10^\circ$  were also  
312 shown to provide reliable measurements (Table 2).

313 The difference between methods in absolute  $d_{AT}$  lengths described here would have significant  
314 implications for the calculation of AT force. For example, the AT force in a healthy adult  
315 population with an ankle plantarflexion moment of 20 N m and a  $d_{AT}$  of 43 mm (measured via  
316 MRI) would be  $\sim 465$  N. However, if the  $d_{AT}$  value measured via DXA replaced the MRI  
317 measure in the equation (e.g. 53 mm) the AT force would be calculated as  $\sim 377$  N, a difference  
318 of  $\sim 88$  N. It is acknowledged though, that investigations in different populations and additional  
319 work would be required before a universal correction factor may be applied (Erskine et al.,  
320 2014). A post hoc power analysis ( $1-\beta$  err prob) of this study was  $<0.99$ , thus confirming that  
321 the results of this study can be generalised to young healthy adult populations.

322 The findings of this study could allow for the use of DXA-derived  $d_{AT}$  measurements to be  
323 used in the calculation of the GM and AT properties. The results may also mean that future

324 research should be cautious when selecting the TE method to determine  $d_{AT}$  (Hashizume et al.,  
325 2016). With popularity of DXA rising in recent years to measure muscle mass and body  
326 composition, it would be beneficial to utilise DXA based  $d_{AT}$  measurements. The ability to  
327 utilise the DXA technique to measure  $d_{AT}$  would allow for researchers to determine muscle-  
328 tendon forces, which would be helpful in illustrating group differences and/or intervention  
329 induced variations in calf ‘muscle strength’. The DXA technique, however, delivers radiation  
330 to participants, with the effective dose estimated to be 56  $\mu\text{Sv}$  with the IVA-HD protocol.  
331 Fortunately, this effective dose is ‘extremely low’ and is well below the maximum  
332 recommended annual dose regarded as safe, i.e. 1,000  $\mu\text{Sv}$  (Njeh et al., 1999). Despite the  
333 ‘extremely low’ radiation, researchers may wish to use DXA in future studies examining  $d_{AT}$   
334 length as this novel protocol is quicker than the MRI technique and DXA is cheaper and more  
335 easily accessible. Studies examining muscle mass refer to DXA as the gold standard  
336 measurement technique and therefore if already being utilised in the assessment of muscle mass  
337 or body composition, researchers will be able to accurately determine  $d_{AT}$  length and therefore  
338 muscle-tendon forces in one laboratory visit.

339 This study utilised 2D imaging in all methods investigated, which needs to be addressed when  
340 comparing its findings to previous work. Hashizume et al. (2012) found that when employing  
341 2D methods to measure  $d_{AT}$  length as opposed to 3D imaging techniques that the  $d_{AT}$  length  
342 will be overestimated. However, as all techniques investigated were 2D, the reliability and  
343 agreement between techniques can be accepted at the 2D level. Further investigation would be  
344 required to examine the agreement between the novel DXA technique and 3D MRI analysis.  
345 Following on from the results of this study, the use of DXA in the assessment of individuals  
346  $d_{AT}$  has been shown to be reliable at rest. Further investigation should explore the measurement  
347 of  $d_{AT}$  during differing isometric muscle contraction intensity at a range of ankle joint angles.

348

349 **Conclusion**

350 This study has illustrated that reliable measurements of  $d_{AT}$  length at rest can be estimated from  
351 the IVA-HD DXA scan protocol. The novel DXA method gave consistently longer  $d_{AT}$  lengths  
352 (19.7-24.9%) at all ankle angles measured ( $-5^\circ$ ,  $0^\circ$ ,  $+10^\circ$ ) compared to the reference MRI  
353 method. However, we have shown the novel DXA and MRI techniques were in strong  
354 agreement irrespective of inter-individual differences in ankle joint dimensions. This finding  
355 provides a novel method in the calculation of AT forces *in vivo* and allows comparisons to be  
356 drawn between existing and future studies.

357

358

359

360

361

362

363

364

365

366

367

368

369

370

371

372

373



374 **Acknowledgements**

375 We would like to extend our gratitude to the Musculoskeletal Science and Sports Medicine  
376 Research Centre at Manchester Metropolitan University for their continued support.

377

378 **Conflict of interests**

379 AJ Buffey - no conflict of interests

380 GL Onambélé-Pearson – no conflict of interests

381 RM Erskine - no conflict of interests

382 DJ Tomlinson - no conflict of interests

383

384 **Data Reference**

385 The datasets generated and/or analysed during the current study will be available in the  
386 Manchester Metropolitan University repository (link will provided upon publication).

387

388

389 **References**

- 390 Alexander, C.F., Lum, I., Reid, S., Clarke, E., Stannage, K., El-Sallam Abd, A., Herbert, R.D.,  
391 Donnelly, C.J., 2017. A simple but reliable method for measuring 3D Achilles tendon moment  
392 arm geometry from a single, static magnetic resonance scan. *J Biomech* 55, 134-138.
- 393 Baxter, J.R., Piazza, S.J., 2018. Plantarflexor moment arms estimated from tendon excursion  
394 in vivo are not strongly correlated with geometric measurements. *J Biomech* 77, 201-205.
- 395 Clarke, E.C., Martin, J.H., d'Entremont, A.G., Pandy, M.G., Wilson, D.R., Herbert, R.D., 2015.  
396 A non-invasive, 3D, dynamic MRI method for measuring muscle moment arms in vivo:  
397 demonstration in the human ankle joint and Achilles tendon. *Med Eng Phys* 37, 93-99.
- 398 Erskine, R.M., Jones, D.A., Williams, A.G., Stewart, C.E., Degens, H., 2010. Resistance  
399 training increases in vivo quadriceps femoris muscle specific tension in young men. *Acta*  
400 *Physiol (Oxf)* 199, 83-89.
- 401 Erskine, R.M., Morse, C.I., Day, S.H., Williams, A.G., Onambele-Pearson, G.L., 2014. The  
402 human patellar tendon moment arm assessed in vivo using dual-energy X-ray absorptiometry.  
403 *J Biomech* 47, 1294-1298.
- 404 Fath, F., Blazeovich, A.J., Waugh, C.M., Miller, S.C., Korff, T., 2010. Direct comparison of in  
405 vivo Achilles tendon moment arms obtained from ultrasound and MR scans. *Journal of applied*  
406 *physiology* 109, 1644-1652.

407 Fletcher, J.R., MacIntosh, B.R., 2018. Estimates of Achilles Tendon Moment Arm Length at  
408 Different Ankle Joint Angles: Effect of Passive Moment. *Journal of applied biomechanics*, 1-  
409 22.

410 Hashizume, S., Fukutani, A., Kusumoto, K., Kurihara, T., Yanagiya, T., 2016. Comparison of  
411 the Achilles tendon moment arms determined using the tendon excursion and three -  
412 dimensional methods. *Physiol Rep*. 2016 Oct 5;4(19):e12967. doi: 10.14814/phy2.12967.  
413 eCollection 2016 Oct.

414 Hashizume, S., Iwanuma, S., Akagi, R., Kanehisa, H., Kawakami, Y., Yanai, T., 2012. In vivo  
415 determination of the Achilles tendon moment arm in three-dimensions. *J Biomech* 45, 409-413.

416 Lee, S.S., Piazza, S.J., 2009. Built for speed: musculoskeletal structure and sprinting ability. *J*  
417 *Exp Biol* 212, 3700-3707.

418 Maganaris, C.N., 2003. Force-length characteristics of the in vivo human gastrocnemius  
419 muscle. *Clin Anat* 16, 215-223.

420 Maganaris, C.N., 2004. Imaging-based estimates of moment arm length in intact human  
421 muscle-tendons. *European journal of applied physiology* 91, 130-139.

422 Maganaris, C.N., Baltzopoulos, V., Sargeant, A.J., 1998. Changes in Achilles tendon moment  
423 arm from rest to maximum isometric plantarflexion: in vivo observations in man. *The Journal*  
424 *of physiology* 510 ( Pt 3), 977-985.

425 Maganaris, C.N., Baltzopoulos, V., Sargeant, A.J., 2000. In vivo measurement-based  
426 estimations of the human Achilles tendon moment arm. *European journal of applied physiology*  
427 83, 363-369.

428 Maganaris, C.N., Paul, J.P., 1999. In vivo human tendon mechanical properties. *The Journal*  
429 *of physiology* 521 Pt 1, 307-313.

430 Muraoka, T., Muramatsu, T., Takeshita, D., Kawakami, Y., Fukunaga, T., 2002. Length change  
431 of human gastrocnemius aponeurosis and tendon during passive joint motion. *Cells Tissues*  
432 *Organs* 171, 260-268.

433 Njeh, C.F., Fuerst, T., Hans, D., Blake, G.M., Genant, H.K., 1999. Radiation exposure in bone  
434 mineral density assessment. *Appl Radiat Isot* 50, 215-236.

435 Onambele-Pearson, G.L., Pearson, S.J., 2012. The magnitude and character of resistance-  
436 training-induced increase in tendon stiffness at old age is gender specific. *Age* 34, 427-438.

437 Rasske, K., Thelen, D.G., Franz, J.R., 2017. Variation in the human Achilles tendon moment  
438 arm during walking. *Comput Methods Biomech Biomed Engin* 20, 201-205.

439 Rugg, S.G., Gregor, R.J., Mandelbaum, B.R., Chiu, L., 1990. In vivo moment arm calculations  
440 at the ankle using magnetic resonance imaging (MRI). *J Biomech* 23, 495-501.

441 Sheehan, F.T., 2012. The 3D in vivo Achilles' tendon moment arm, quantified during active  
442 muscle control and compared across sexes. *J Biomech* 45, 225-230.

443 Tomlinson, D.J., Erskine, R.M., Winwood, K., Morse, C.I., Onambele, G.L., 2014. Obesity  
444 decreases both whole muscle and fascicle strength in young females but only exacerbates the  
445 aging-related whole muscle level asthenia. *Physiological reports* 2.

446 Wilson, D.L., Zhu, Q., Duerk, J.L., Mansour, J.M., Kilgore, K., Crago, P.E., 1999. Estimation  
447 of tendon moment arms from three-dimensional magnetic resonance images. *Ann Biomed Eng*  
448 27, 247-256.

449 World Medical, A., 2013. World Medical Association Declaration of Helsinki: ethical  
450 principles for medical research involving human subjects. *Jama* 310, 2191-2194.

451

452

453

454

455

456

457

458

459

460

461

462

463

464

465

466 **Tables**

467 **Table 1.** The Achilles tendon moment arm ( $d_{AT}$ ) length measured using dual energy x-ray  
 468 absorptiometry (DXA) and magnetic resonance imaging (MRI) at the three predetermined  
 469 ankle angles and tendon excursion (TE) at 0°.

	DXA	TE	MRI	<i>p-Value</i>
$d_{AT}$ (-5°) (mm)	50.9±4.5	-	41.5±3.4	<0.001
$d_{AT}$ (0°) (mm) (*)	53.8±5.0	29.5±6.2	43.3±3.6	<0.001
$d_{AT}$ (10°) (mm)	56.7±5.8	-	45.4±3.8	<0.001

470 Data are reported mean±SD. (\* denotes that the *p*-value reported was from the Bonferroni  
 471 corrected post hoc).

472

473

474

475

476

477

478

479

480

481

482

483

484

485

486

487 **Table 2.** Achilles tendon moment arm ( $d_{AT}$ ) measurement along with the CV (%) between the  
 488 two datasets (test-retest) and ICC for the dual energy x-ray absorptiometry (DXA) method.

	DXA (-5°)	DXA (0°)	DXA (10°)
$d_{AT}$ (mm) Test 1	50.9±4.5	53.8±5.0	56.7±5.8
$d_{AT}$ (mm) Test 2	51.4±4.8	53.4±4.3	58.2±6.7
CV (%)	2.15	1.38	3.01
ICC (Lower CL - Upper CL) *	0.89 (0.68-0.97)	0.96 (0.86-0.99)	0.76 (0.38-0.92)
ICC (Lower CL - Upper CL) **	0.89 (0.66-0.97)	0.96 (0.86-0.99)	0.77 (0.37-0.93)

489 (\* indicates absolute agreement and \*\* indicates consistency).

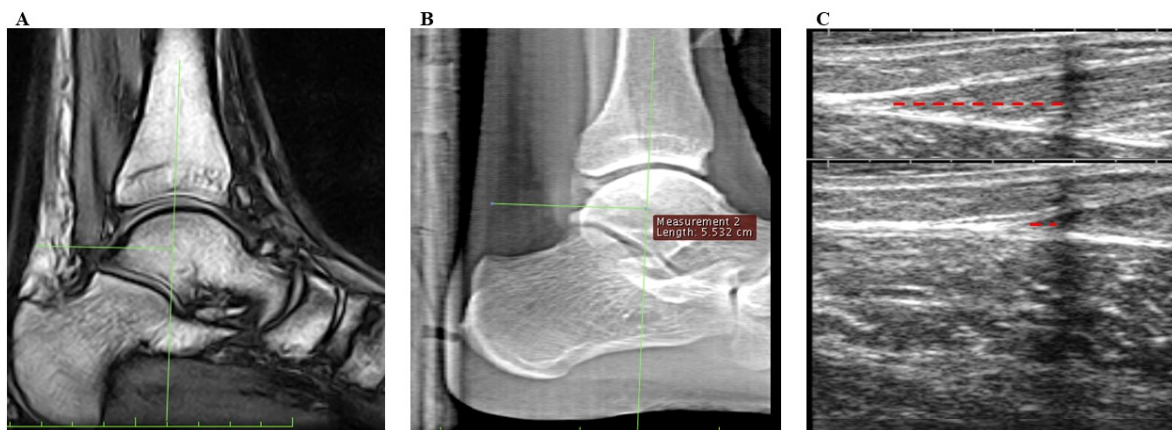
490  
 491  
 492  
 493  
 494  
 495  
 496  
 497  
 498  
 499  
 500  
 501  
 502

503 **Figure**



504

505 **Figure 1.** Representative images illustrating (A) the lower limb positioning within the (A)  
506 magnetic resonance imaging, (B) dual energy x-ray absorptiometry (DXA) and (C) tendon  
507 excursion protocol.

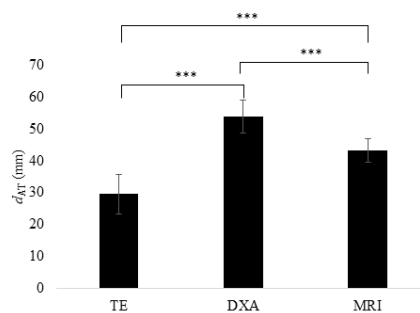


508

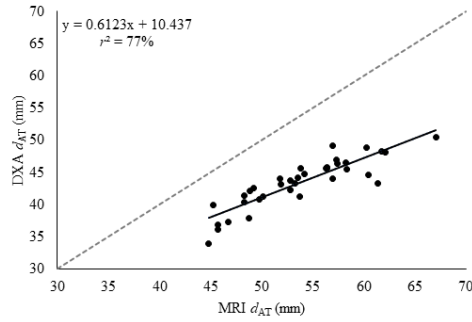
509 **Figure 2.** Representative images demonstrating: (A) the anatomical landmarks used to measure  
510 Achilles tendon (AT) moment arm ( $d_{AT}$ ) in the MRI COR method. The near horizontal green



511 line represents the measurement of the individuals  $d_{AT}$  from the AT line of action (straight  
512 white line) to the estimated centre of the calcaneal joint. (B) The measurement process of a  
513 single 2D dual energy x-ray absorptiometry (DXA) scan for the analysis of  $d_{AT}$ . The near  
514 horizontal green line represents the measurement of the individuals  $d_{AT}$  from the AT line of  
515 action to the estimated centre of the calcaneal joint and (C) illustrating tendon elongation  
516 measured during the tendon excursion technique. The dashed red lines represent the movement  
517 of the gastrocnemius medialis muscle-tendon junction during passive rotation of the ankle. The  
518 echo absorptive is shown as the faint black line through the ultrasound image.  
519



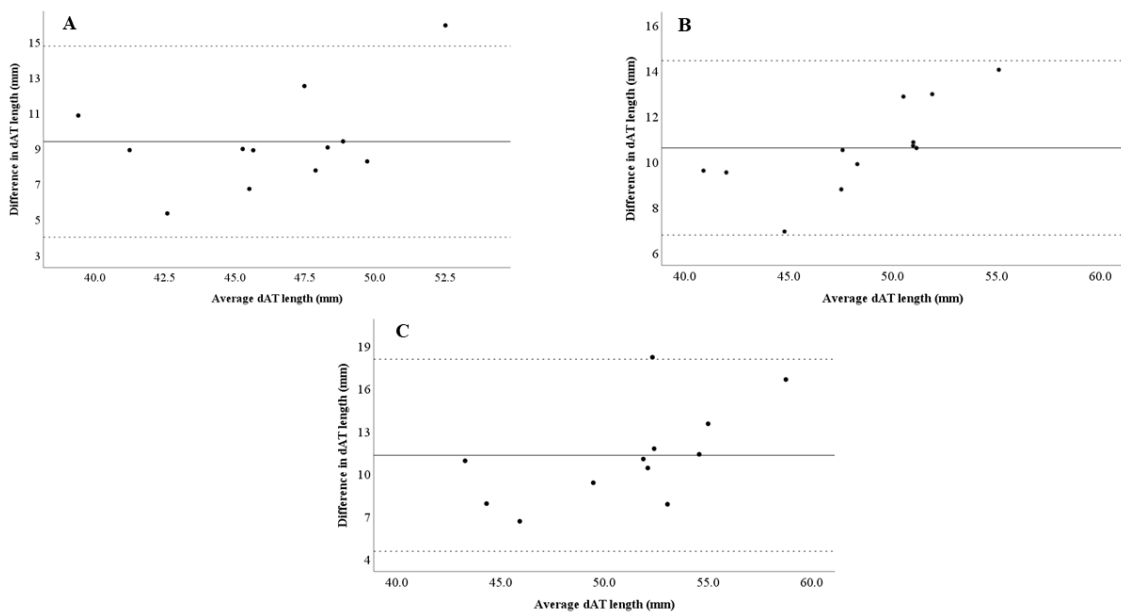
520  
521 **Figure 3.** Displaying Achilles tendon moment arm ( $d_{AT}$ ) length at  $0^\circ$  ankle angle measured by  
522 tendon excursion (TE), dual energy x-ray absorptiometry (DXA) and magnetic resonance  
523 imaging (MRI). \*\*\* denotes a significant difference between tendon excursion (TE) and dual  
524 energy x-ray absorptiometry (DXA) measurements ( $p<0.001$ ); between DXA and MRI  
525 ( $p<0.001$ ); \*\*\* and between TE and MRI ( $p<0.001$ ).  
526  
527



529

530 **Figure 4.** Displaying the Pearson correlation between measurements attained using the dual  
531 energy x-ray absorptiometry (DXA) and magnetic resonance imaging (MRI) techniques  
532 comparing measurements taken at all ankle angles (solid black line=linear correlation ( $r=0.878$ ,  
533  $p<0.001$ ); dashed line=line of identity;  $n=12$ ).

534



535

536 **Figure 5** Bland-Altman plots demonstrating: (A) the systematic bias (+9.4 mm) when  
537 measuring  $d_{AT}$  at  $-5^\circ$  ankle angle when measured by the novel dual energy x-ray absorptiometry  
538 (DXA) technique compared to the magnetic resonance imaging (MRI) protocol. (B) The  
539 systematic bias (+10.4 mm) when measuring  $d_{AT}$  at  $0^\circ$  ankle angle when measured by the novel  
540 DXA technique compared to the MRI protocol. (C) The systematic bias (+11.3 mm) when  
541 measuring  $d_{AT}$  at  $10^\circ$  ankle angle when measured by the novel DXA technique compared to the  
542 MRI protocol. Solid line=mean differences; dashed lines=limits of agreement.  
543